Thermal properties of a raw earth-flax fibers building material

Ichrak Hamrouni, Habib Jalili, Tariq Ouahbi, Said Taibi, Mehrez Jamei, Abdelkader Mabrouk

Construction and Building Materials 423 (2024) 135828

Contents lists available at ScienceDirect

Construction and Building Materials

journal homepage: www.elsevier.com/locate/conbuildmat

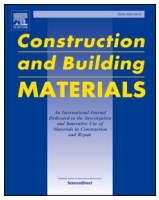

Thermal properties of a raw earth-flax fibers building material

Ichrak Hamrouni [a,b,1], Habib Jalili [a,2], Tariq Ouahbi [a,*,3], Said Taibi [a,4], Mehrez Jamei [c,5], Abdelkader Mabrouk [c,6]

[a] Normandie University, UNIHAVRE, Laboratory of Waves and Complex Media, UMR, Le Havre 6294 CNRS, France
[b] Tunis El Manar University, National Engineering School of Tunis, Civil Engineering Laboratory, Le Belvedere, Tunis 1002, Tunisia
[c] Northern Border University, Engineering College, Civil Engineering Department, Arar, Saudi Arabia

ARTICLE INFO

Keywords:
Thermal conductivity
Heat capacity
Raw earth
Flax fibers
Composite material
Density
Arrangement
Water content
Temperature

ABSTRACT

The aim of this paper is to investigate the thermal behavior of composite building materials comprised of silt and flax fibers, considering various initial conditions. The experiments were conducted on flax fibers alone, examining factors such as moisture content variation, fibers arrangement, and density. Subsequently, the thermal properties of the earth-flax fiber composite were studied, taking into account the influence of water content and fibers mass content. The thermal properties of both flax fibers and raw earth-flax fibers composite specimens were determined using the experimental unsteady-state method. The results indicate that the thermal conductivity and heat capacity of flax fibers increase with density, temperature, and moisture content. Regardless of fibers density and arrangement of fibers, linear relationships have been established for both thermal conductivity and heat capacity as functions of temperature. Additionally, it was demonstrated that the heat capacity and the thermal conductivity increase with water content, regardless of the percentage of added fibers. Moreover, mixing randomly flax fibers with compacted raw earth material has improved the thermal properties of the composite. This improvement pertains to its insulating capacity, ability to store heat, and, subsequently, its contribution to the thermal comfort provided by such earth composite material when used as a building material.

1. Introduction

For thousands of years, human civilizations have used raw earth as a basic building material. According to the International Center for Earthen Construction, one-third of the world's population lives in raw earth habitats [17,19,25]. Nowadays, there has been a renewed interest in this material owing to its mechanical and hydrothermal benefits (see, for instance, [9]; [21,42,6]). Regarding the hygrothermal aspect, numerous studies have shown that raw earth-based materials have been considered effective in reducing energy consumption in construction and enhancing the hygrothermal comfort of buildings [25,35,42]. They are manufactured from natural raw materials—local soils and agricultural products—and require simple in situ production processes, making them environmentally friendly and non-polluting. Earth construction materials can be found in various forms, including adobes, compressed earth bricks, concrete, and cob [22,26,39,41,42,50,6,7]. Nevertheless, the choice of a raw earth-based eco-material must adhere to specific criteria regarding allowable mechanical resistance [17,19], durability, rigidity/ductility, as well as heat and moisture transfer properties.

Previously, research on bio-based and earth-based materials has been essentially focused on mechanical performance [6,38,47] and shrinkage [43,44]. However, these materials offer additional benefits that necessitate investigation, particularly those related to hygrothermal properties. Indeed, literature has recently begun to mention the positive impact of earth on hygrothermal comfort, prompting studies to thoroughly examine the properties of composite earth materials [10,18,25,42].

Recently, researchers have shown a growing interest in the thermal

* Corresponding author.
E-mail address: tariq.ouahbi@univ-lehavre.fr (T. Ouahbi).
[1] ORCID: 0000-0002-7263-7217
[2] ORCID: 0000-0002-4215-1646
[3] ORCID: 0000-0002-2573-3230
[4] ORCID: 0000-0002-1221-2997
[5] ORCID: 0000-0002-9430-3920
[6] ORCID: 0000-0001-9712-8067

https://doi.org/10.1016/j.conbuildmat.2024.135828
Received 7 January 2024; Received in revised form 3 March 2024; Accepted 6 March 2024

properties of vegetal fibers [1,10,23,42,6], as well as in raw earth-vegetal fibers construction materials (Hall & Allison, 2009; [40, 50,42,6]). In this context, several researchers have conducted experimental studies to measure the thermal conductivity of vegetal fibers. As a non-exhaustive example, [23] conducted a comparison of the thermal conductivity, thermal diffusivity, and specific heat capacity properties of different types of fibers. It was demonstrated that straw fibers exhibit favorable thermal properties compared to other vegetal fibers, such as thatch. For instance, for straw fibers with a density of 60 kg/m^3, the thermal conductivity, thermal diffusivity, and specific heat capacity were recorded as 0.067 W/ (m. K), 18.2×10^7 m^2/s and 600 J/ (kg. K), respectively. Additionally, studying the role of fibers density on thermal conductivity, Vaitkus [46] concluded that this property decreases with an increase in fibers density. For example, 1) regarding chopped flax fibers, the thermal conductivity varies from 0.052 to 0.045 W/ (m. K) with an increase in density from 40 to 100 kg/m^3. 2) Regarding combed longue flax fibers, the thermal conductivity decreases from 0.044 to 0.034 W/ (m.K) as the density increases from 40 to 100 kg/m^3. Brouard et al. [10] measured the thermal conductivity of rape straw and sunflower fibers. For densities ranging from 15.9 to 129.3 kg/m^3, the thermal conductivity of both two types of fibers varied from 0.036 to 0.053 W/ (m. K). Additionally, Abbas et al. [1] examined the thermal conductivity of hemp and sunflower using a transient measurement method. The results indicate that the thermal conductivity of hemp is approximately 0.07 W/ (m. K) at a density of 100 kg/m^3, while for sunflower, it is around 0.05 W/ (m. K) at a density of 14 kg/m^3. The thermal conductivity value obtained for sunflower is close to findings by Magniont [33] and Chabannes et al. [13]. These results demonstrate comparability to synthetic insulation materials such as expanded polystyrene or glass wool, which typically exhibit thermal conductivities ranging from 0.03 and 0.04 W/ (m. K).

Regarding the thermal properties of composite materials, particularly raw earth composites involving fibers-matrix mixing, several studies [26,42,6,7] have demonstrated the impact of water content on thermal conductivity and heat capacity. Their results generally indicate that both parameters increase linearly with water content. For instance, Hibouche [26] measured the thermal conductivity of a raw earth concrete comprising silt, mineral binders (cement and lime), and natural flax fibers as a function of water content. Operating in the steady-state, the thermal conductivity increases linearly from 0.564 to 1.167 W/ (m. K) as the water content ranges from 0% to 29%. Furthermore, using the unsteady state method, Hibouche, [26] has demonstrated that the thermal conductivity and the heat capacity vary linearly, respectively, within the same ranges of water content, from 0.4 to 1.4 W/ (m. K) and from 1.5 to 2.9 MJ/ (m^3. K). The corresponding raw earth concrete exhibits approximately three times more insulation than cement concrete. Moreover, numerous researchers examining the hydrothermal behavior of raw earth-vegetal fibers composites have evaluated the impact of vegetal fibers content on the hydrothermal properties. For instance, Phung et al. [42] examined the influence of water and fibers contents on the thermal conductivity of various cob formulations. Two types of soil were used: one comprised 26.7% gravel, 40.5% sand, and 2.8% silt, while the other consisted of 26% gravel, 35.5% sand, and 8.5% silt and clay. Straw fibers contents ranging from 0% to 3% were added to these soils. The results revealed that, for both composite materials, thermal conductivity decreased with added fibers content but increased with increased water content. At a fibers content of 3%, the thermal conductivity was measured at 0.65 W/ (m. K) for the first soil and 0.59 W/(m. K) for the second soil. They concluded that the second material might offer better thermal comfort for construction purposes. Furthermore, Mazhoud et al. [35] examined the impact of clay stabilization and hemp content on hygrothermal properties. Various factors were identified, such as the sorption isotherm, moisture buffering capacity, and thermal conductivity. From the results, for the two types of binders, the thermal conductivity ranges from 0.089 to 0.12 W/ (m. K) in the dry state and increases linearly versus density and water content. They conclude that these composites exhibit high thermal qualities, making them suitable for insulation. Other authors, such as Azil et al. [6], evaluated the impact of temperature, relative humidity (RH), and wind velocity variations on the thermal conductivity of cob and light-earth materials in a climatic chamber under winter and summer conditions. The thermal conductivity measurements conducted under summer and winter conditions established correlations between the thermal conductivity, density, and water content of the two studied materials under evaluation. It decreased as the water content reduced, reaching values of 1.31–0.48 W/ (m. K) in summer (with temperatures ranging from 0 to 40°C) and from 1.27 to 0.58 W/ (m. K) in winter (temperature ranges from −10–20°C). They concluded that the kinetics of thermal conductivity in relation to density and water content exhibit similarities in summer and winter conditions.

Reviewing the literature on biosourced materials reveals that very few authors have studied the thermal properties of plant/vegetal fibers. According to the author's knowledge, the role of fibers disposition and arrangement (longitudinal and random) on heat transfer properties has not yet been explored, and consequently, the impact of adding fibers on the thermal properties of raw earth composite building materials remains unexamined. Subsequently, this study focuses on the thermal properties of a raw earth-flax fibers composite using a transient transfer method. First, the thermal conductivity and the heat capacity of flax fibers alone were measured, taking into account the impact of water content, temperature, arrangement, and density. Then, these same thermal properties were measured for the raw earth-flax fibers composite, considering the influence of both water and fibers contents separately.

2. Materials and methods

2.1. Materials

2.1.1. Raw earth

The raw earth material (see Fig. 1) is a soil abundant in Gonfreville l'Orcher, Le Havre, Normandy, in France. Two methods were employed to determine the particle size distribution of this soil: sedimentary analysis for fine particles smaller than 0.075 mm in diameter and sieve grain size analysis for coarser particles ranging from 0.075 mm to 100 mm. The soil comprises approximately 67% sand (ranging from 0.06 mm to 2 mm), about 25% silt (ranging from 2 μm to 60 μm), and 8% gravel (< 2 mm). Additionally, it is classified as silty sand SL (SM) soil according to the Unified Soil Classification System (USCS) and the ASTM D2487–11 standard.

Fig. 1. Silty-Sand soil from the field.

2.2. Flax fibers

The fibers are natural, cut to 70 mm in length (see Fig. 2), dried, and stored under ambient conditions. The mechanical properties of these fibers are as follows: Young's modulus E = 40–80 GPa, ultimate strain σ_u = 2.4–3.3%, and ultimate stress σ_u = 800–2000 MPa [17,19].

3. Samples preparation

3.1. Flax fibers samples

A cylindrical PVC tube with a constant diameter (d) of 40 mm and length (l) of 70 mm was utilized for flax fibers specimens to achieve various densities ranging from 100 to 400 kg/m^3. In this context, the various weights of dried flax fibers were measured, and then the density of the specimens was calculated using the constant volume of the PVC tube ($V = \frac{\pi \times d^2}{4} \times l$). With a constant volume and varying mass of fibers (m), the density was calculated by dividing the mass of fibers in kg by the volume (V) of PVC tube, $\rho = \frac{m}{V}$ (kg/m^3). Two different arrangements of the flax fibers in the constant volume of the PVC tube —longitudinal and random arrangements— were considered across different densities (see Table 1). Flax fibers were compacted and fitted into the PVC tube with these various arrangements and densities.

3.2. Raw earth-flax fibers composite samples

The raw earth-flax fibers samples were prepared through static compaction in a Proctor mold. The fibers are added randomly, with a content by mass ranging from 0% to 3%. The samples were with a fixed diameter of 100 mm and a thickness of 50 mm. They were compacted at a dry density of γ_d=17 kN/m^3 and an optimum moisture content (OMC) of 14% (see Table 1). The physical characteristics of the samples, including density, water content, and porosity, were deduced from the measurement of the sample total volume by immersed weighing using non-wetting Kerdane Oil. By knowing the volume of the solid matrix, volume of the pores could be deduced [8].

Starting from the initial compaction state (γ_d = 17 kN/m^3 and w = 14%), the samples were wetted until full saturation (by calculating the degree of saturation and then deducing the moisture content at saturation, w_{sat}). Indeed, the degree of saturation is defined by the following Eq. 1:

Fig. 2. Flax fibers with the length of 70 mm.

$$S_r = \frac{w \times G_s}{e} \quad (1)$$

Assuming that γ_d is constant and given the specific gravity of the soil $G_s = \frac{\gamma_s}{\gamma_w}$, the void ratio $e = \frac{\gamma_s}{\gamma_d} - 1$ was obtained, and then the degree of saturation was determined. Clearly, the moisture content at saturation, w_{sat}, corresponds to $S_r = 1$. Fig. 3 represents the path followed, $S_r = f(w)$, to obtain the water content during the experiment until full saturation is reached. Subsequently, starting from the moisture content at saturation, the specimens were dried in the oven at a fixed temperature (drying path, Fig. 4) to achieve the desired water content, which was continuously measured.

3.3. Experimental methods

For measuring the thermal properties, including thermal conductivity and heat capacity, of both flax fibers alone and raw earth-flax fibers samples, the thermal unsteady-state method was used. This method is often used for homogeneous and heterogeneous materials with high moisture content, and it adheres to the standard **ISO 8894–2 1990**. The thermal unsteady-state method is based on heat dissipation analysis and entails introducing a heat source into the sample (either flax fibers or raw earth-flax fibers samples) to generate a heat pulse within it. Initially, the temperature in the specimen was set at a fixed temperature of T_0, and then its variation within the sample was recorded throughout the experiment. The variation of temperature within the sample was recorded, and the recording ceased upon reaching the initial temperature T_0 once again. The advantage of this method, compared to the steady-state method, lies in the instantaneous nature of the results, allowing for the tracking of heat exchange capacity over time. The thermal conductivity and heat capacity of the flax fibers and raw earth-flax fibers materials were measured using a commercial analyzer of the METER Group company (TEMPOS, Meter Group, Inc., Pullman, WA, USA, accuracy: 10%). The TEMPOS portable device used for these thermal measurements (as shown in Fig. 5) is a data acquisition unit equipped with different sensors (SH-3, TR-3, KS-3, and RK-3) depending on the type of the studied material. For this study, the SH-3 dual-needle sensor was used for both the raw earth and the composite raw earth-flax fibers samples. Meanwhile, the KS-3 single-needle sensor was used for analyzing the thermal properties of flax fibers samples. The characteristics of the SH-3 and KS-3 sensors are summarized in Table 2.

These needles are to be inserted into the samples and serve a dual purpose, functioning as both temperature sensors and heat sources simultaneously (Fig. 6.a and Fig. 6.b). Firstly, an electric current is applied through the sensor to heat the sample. The temperature, measured by a thermocouple installed in the middle of this sensor, is recorded as a function of time. Then, the thermal conductivity of the sample is calculated from the temperature variation over time and the heat flux. After this, the thermal diffusivity and the heat capacity are deduced. The TEMPOS device maintains minimal heating times due to water movement and free convection, thereby ensuring a short duration for each measurement according to specific methods. The test duration is approximately 150 seconds, divided as shown in Fig. 7. These algorithms and theories are derived from the research conducted by Knight et al. [31], who explain the transformation of Blackwell's solution into the time domain. This work has been extensively utilized in TEMPOS devices to produce improved algorithms, including both single-needle and dual-needle algorithms.

In the single-needle algorithm, a linear heat source (KS-3 thermal needle) is introduced into the sample, resulting in an increase in temperature from an initial temperature T_0 at a distance r from the axis of the source. The equation used for single-needle sensors,

$$\Delta T = T - T_0 = \left(\frac{q}{4\pi \quad \lambda}\right)\ln(t) + C \quad (2)$$

Table 1
Different cases studied for the measurement of thermal properties.

Samples	Properties	Dimensions
Raw earth Compacted silty-sand	**Density γ_d (kN/m^3)** 17 Water content *w* varies from 0% to 20%	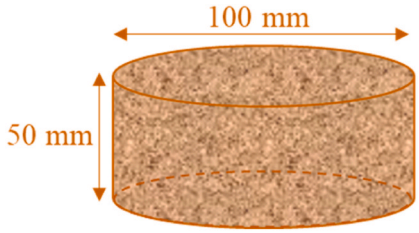
Earth-fibers mixture Silty-sand reinforced with random flax fibers content of 1% and 3%	**Density γ_d (kN/m^3)** 17 *1% of fibers* Water content *w* varies from 0% to 23% *3% of fibers* Water content varies from 0% to 26%	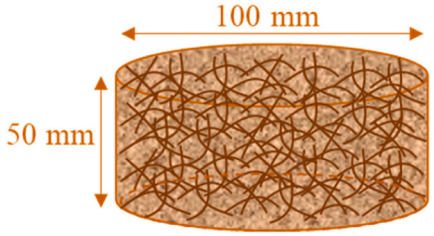
Flax fibers alone Random arrangement	**Density γ_d (kN/m^3)** 100, 200,300 and 400	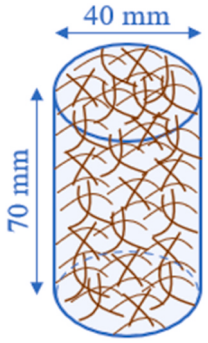
Flax fibers alone Longitudinal arrangement	**Density γ_d (kN/m^3)** 100, 200,300 and 400	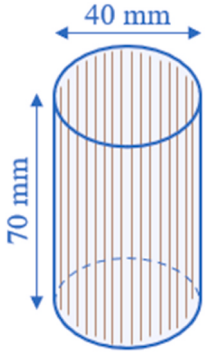

Where T (K) and T_0 (K) denote the temperature and initial temperature, respectively. *q* (W/ m), λ (W/ (m. K)) represent the heat flux and thermal conductivity, respectively, while *t* (s) signifies time. Eq. 2 illustrates that the conductivity is proportional to the inverse of the slope when the temperature difference (ΔT) is plotted versus $\ln(t)$. The values of λ, and C are determined by least squares [34].

In the dual-needle algorithm, heat is applied from the heated needle for a set heating time after initialization, $t_h = 30s$, and the temperature is measured in the monitoring needle 6 mm away during both the heating and cooling periods following heating. The monitored temperature data are fitted to Eq. 3 and Eq. 4 using a least squares procedure.

$$\Delta T = \left(\frac{q}{4\pi\lambda}\right) Ei\left(\frac{-r^2}{4Dt}\right) .t \leq t_h \tag{3}$$

$$\Delta T = \left(\frac{q}{4\pi\lambda}\right)\left\{Ei\left[\frac{-r^2}{4D(t-t_h)}\right] - Ei\left[\frac{-r^2}{4Dt}\right]\right\}., t \geq t_h \tag{4}$$

Where ΔT is the temperature rise at the measuring needle, q is the heat input at the heated needle (W/ m), λ represents the thermal conductivity (W/ (m. K)), r (m) is the distance from the heated needle to the measuring needle (m), D is the thermal diffusivity ($m^2.s^{-1}$), t_h is the heating time (s), and Ei is the exponential integral, approximated using polynomials [2].

From the experiment, the values of q, r, t, and t_h are known, enabling to solve the equations for thermal conductivity, λ and thermal diffusivity, D. Subsequently, we search for the value of D that minimizes the squared differences between measured and modeled temperatures. This method yields the global minimum and, if structured correctly, is as efficient as traditional nonlinear least squares methods. Once λ and D are

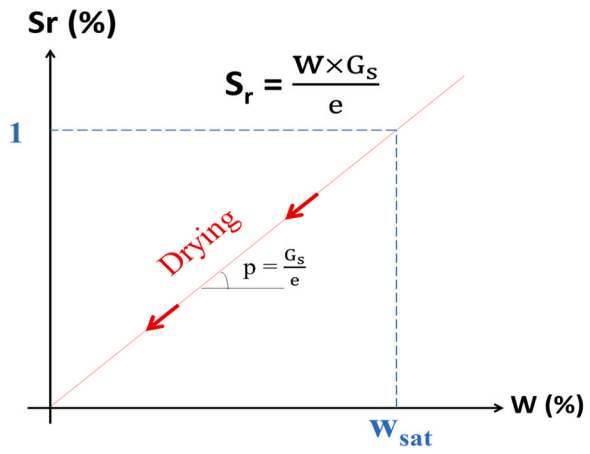

Fig. 3. Degree of saturation evolution versus water content.

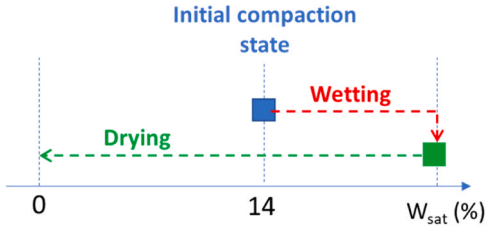

Fig. 4. Wetting/Drying processes for varying the water content of raw earth – flax fibers samples.

Fig. 5. The TEMPOS thermal properties analyzer with KS-3 and SH-3 sensors.

Table 2
Sensor's characteristics.

SH-3 dual-needle sensor		KS-3 single-needle sensor	
Dimensions		**Dimensions**	
1.3 mm diameter × 30 mm length 6 mm spacing between needles		1.3 mm diameter × 60 mm length	
Type of materials		**Type of materials**	
Solid and granular materials		Insulating materials	
Conductivity		**Conductivity**	
Range	0.02–2.00 W/ (m. K)	**Range**	0.1–4.0 W/ (m. K)
Accuracy	±10% from 0.02 to 2.0 W/ (m. K)	**Accuracy**	±10% from 0.1 to 4.0 W/ (m. K)
Heat capacity (SH-3 dual-needle sensor)			
Range		0.5–4.2 MJ/ (m^3. K)	
Accuracy		±10% at conductivities above 0.1 W/ (m. K)	

determined, the volumetric specific heat capacity, c (MJ/ (m^3. K)) can be calculated by Eq. 5.

$$c = \frac{\lambda}{D} \tag{5}$$

4. Results and discussions

4.1. Flax fibers

4.1.1. Thermal conductivity of flax fibers

4.1.1.1. Effect of water content on thermal conductivity for different densities of fibers. The thermal conductivity λ [W/ (m. K)] of flax fibers was measured as a function of water content for different densities. To prepare samples with different water contents, the flax fibers were first saturated and then subjected to centrifugation to speed up the drying process. As a first step, a calibration curve correlating the fibers' water content with centrifugation speed was established, as demonstrated in Fig. 8. This calibration allows for the control of the fibers' arrangement with different initial water contents. Subsequently, using the TEMPOS thermal analyzer described in section II.3, the thermal conductivity of flax fibers at the desired water content was measured. Fig. 9 illustrates that the thermal conductivity increases linearly with water content, regardless of the fibers' density. For instance, in the case of fibers with a density of 400 kg/m^3, the thermal conductivity increases from 0.067 W/ (m. K) to 0.36 W/ (m. K) with a slope of 2.9×10^{-4} W/ (m. K). Indeed, the higher the moisture content of the fibers, the more heat they conduct, since the thermal conductivity of water is approximately 0.62 W/ (m. K) [29], whereas that of dry fibers is approximately 0.0668 W/ (m. K).

Moreover, the slope ($\frac{\Delta\lambda}{\Delta w}$) for a linear variation of thermal conductivity as a function of the water content increases with the fibers' density. It varies from 3.4×10^{-4} to 2.93×10^{-3} W/ (m. K) when the density increases from 100 to 400 kg/m^3. These results highlighted both the effects of water content and density on heat diffusion. For high densities of flax fibers, the dependence of thermal conductivity on water content is more sensitive.

Additionally, denser flax fibers conduct heat more effectively for a given water content (as shown in Fig. 10). For instance, at a water content of 60%, the thermal conductivity increases from 0.058 W/ (m. K) to 0.24 W/ (m. K) as the density varies from 100 kg/m^3 to 400 kg/m^3. This occurs because there is less void space between fibers, leading to decreased porosity and fewer air gaps as the density increases. However, since air is a good insulator (λ = 0.025 W/ (m. K), [29]), compared to the flax fibers, the denser fibers conduct heat more efficiently.

4.1.2. Effect of the initial temperature on the thermal conductivity of the fibers

To evaluate the impact of the mean temperature across the sample on the heat diffusion capacity of flax fibers, tests were conducted to measure the thermal conductivity λ, at various temperatures, densities, and fibers arrangements. The flax fibers samples were prepared with densities ranging from 100 to 400 kg/m^3 and then placed in a temperature-controlled climate chamber. Once their temperature stabilized, the thermal conductivity was measured. The temperature ranged from 299.15 K to 328.15 K, and two arrangements of fibers, random and longitudinal, were considered for these tests (see Table 1). Fig. 11 and Fig. 12 demonstrate that, regardless of the density and arrangement, the variation of the thermal conductivity increases with the mean temperature following a linear formula presented in Eq. 6. This equation depicts a consistent slope of 0.0003, irrespective of the fibers' density and arrangement. The slope of this relation (a) is an intrinsic physical parameter that characterizes the conductive thermal behavior of flax fibers.

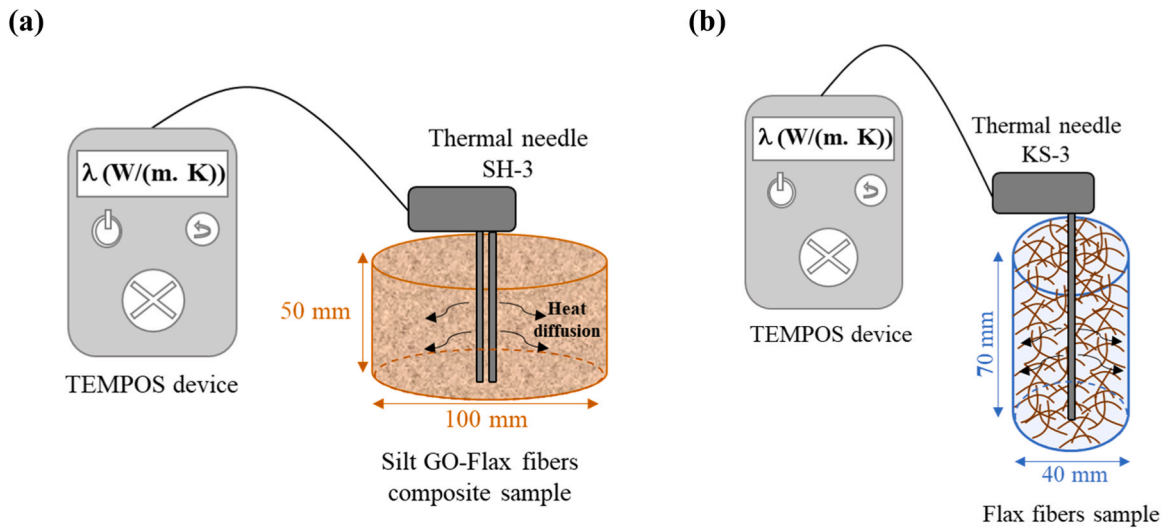

Fig. 6. Shema of the thermal properties measuring of: **(a)** Raw earth-flax fibers, **(b)** Flax fibers alone with random arrangement.

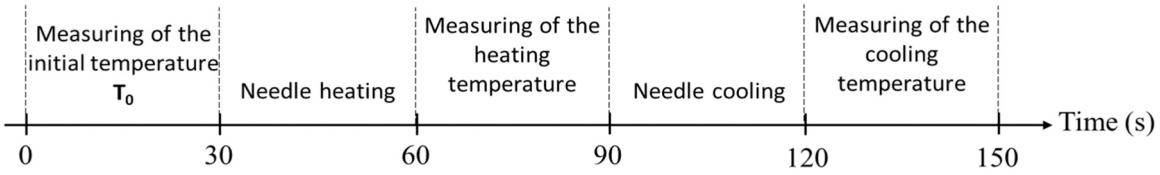

Fig. 7. The duration of the different steps of measuring thermal properties with the transient method.

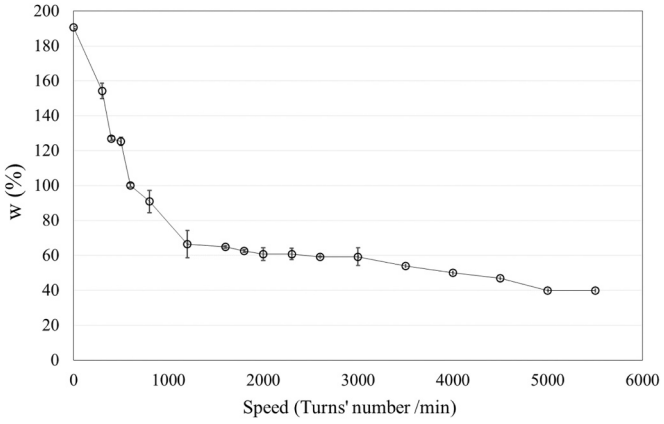

Fig. 8. Calibration curve of fibers water content versus centrifugation speed.

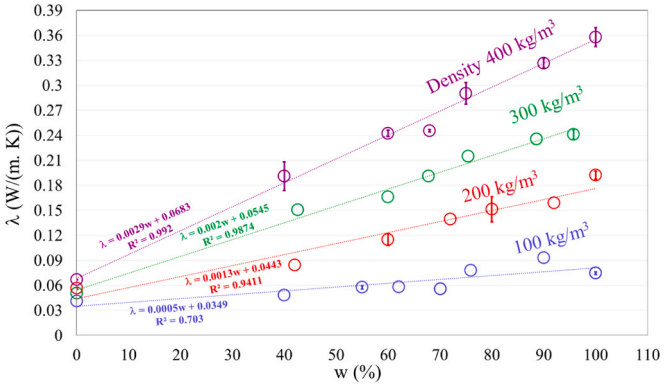

Fig. 9. Flax fibers thermal conductivity evolution versus water content.

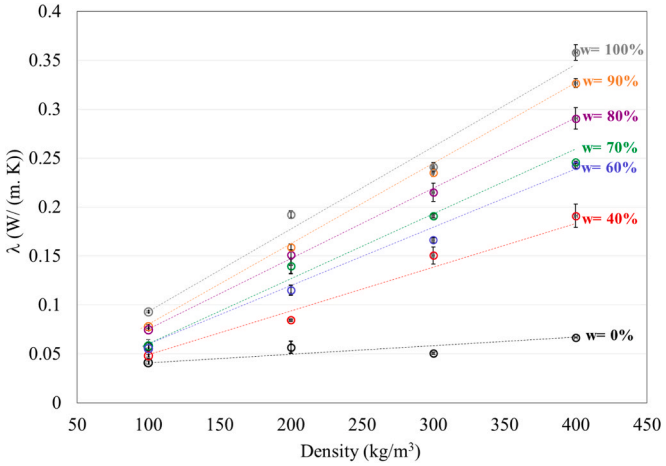

Fig. 10. Flax fibers thermal conductivity evolution versus the density.

$$\lambda = \lambda_0(1 + b \quad T) \tag{6}$$

- λ_0: Thermal conductivity at initial temperature of fibers
- $b = \frac{a}{\lambda_0}$ [K]
- a = 0.0003: Slope of the curve [W/m].

The effect of temperature on thermal conductivity can be explained by the significant volume of air in the flax fibers. As the mean temperature increases, the kinetic energy levels of air molecules intensify. This contributes to a stronger convective heat transfer mechanism, which is expected to vary significantly with temperature in parallel with heat transfers by conduction [15,30,32,45,49]. Indeed, as shown in Fig. 13, researchers also observed similar behavior in different types of fibers,

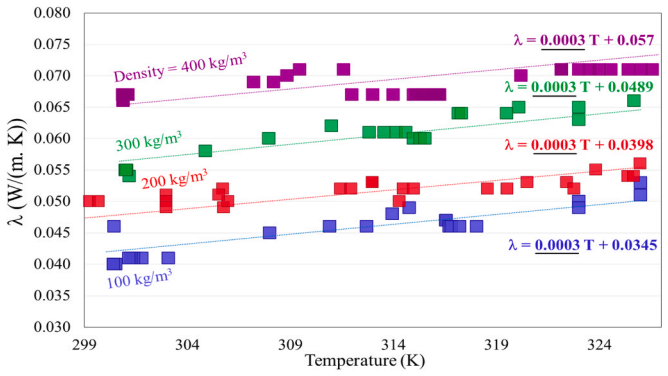

Fig. 11. Thermal conductivity evolution as a function of temperature for random arrangement.

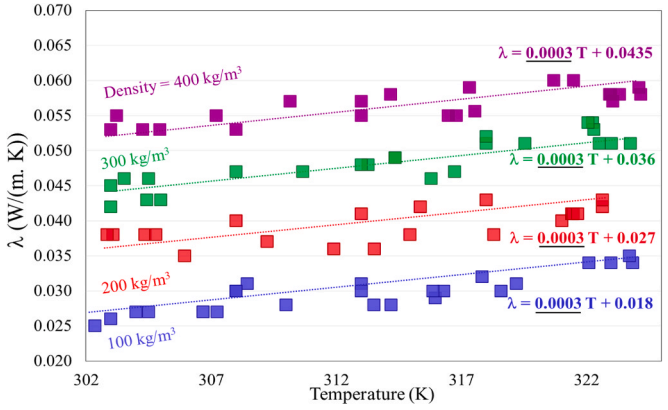

Fig. 12. Thermal conductivity evolution versus a mean temperature for longitudinal arrangement.

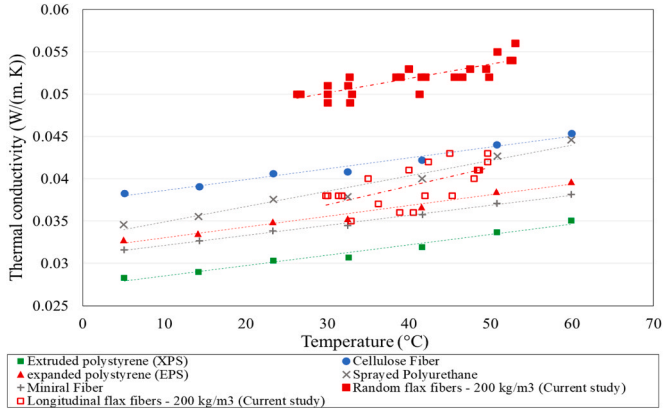

Fig. 13. Comparison of the thermal conductivity of flax fibers with that of insulating materials in the literature [49].

wherein thermal conductivity increases linearly with temperature.

Upon comparing the thermal conductivity of random fibers with that of longitudinal fibers across various densities, ranging from 100 to 400 kg/m^3 (Fig. 14. a and Fig. 14. b), it becomes evident that regardless of the density, random fibers exhibit higher thermal conductivity than longitudinal fibers. This discrepancy arises because, in the case of a random arrangement, flax fibers are more densely compacted compared to the longitudinal arrangements, allowing for greater heat diffusion. This is due to the higher thermal conductivity of individual fibers compared to the air.

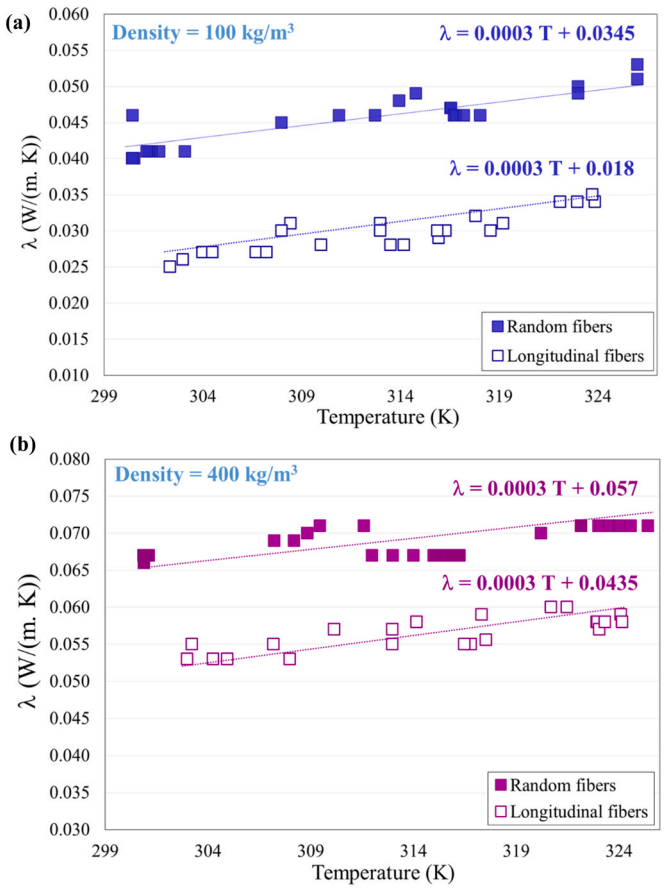

Fig. 14. Comparison of thermal conductivity results of random and longitudinal fibers for densities: (a) 100 kg/m^3 and (b) 400 kg/m^3.

4.2. Heat capacity of flax fibers

4.2.1. Effect of water content and density of fibers on heat capacity

The evolution of heat capacity c [MJ/ (m^3. K)] versus water content is depicted in Fig. 15. A linear relationship is observed regardless of the fibers' density and moisture content. For fibers with a density of 100 kg/ m^3, the heat capacity increases from 0.41 to 2.47 MJ/ (m^3. K) as the water content varies from 0% to 100%, respectively. Conversely, in the case of a density of 400 kg/m^3, it increases from 0.57 to 3.63 MJ/ (m^3. K) for the same range of moisture contents. Additionally, for a given moisture content, heat capacity increases in denser fibers. Decreased air

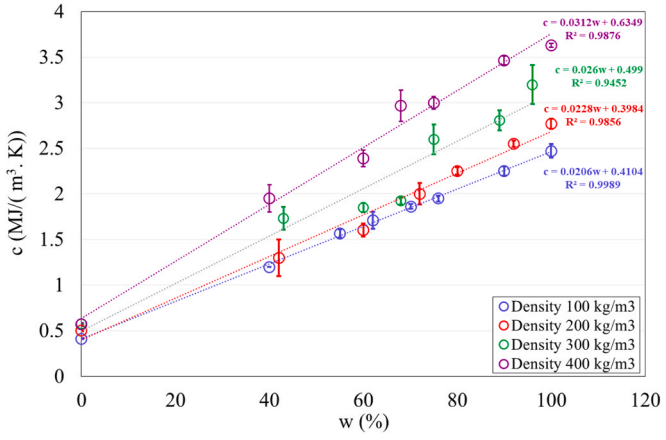

Fig. 15. Heat capacity of flax fibers evolution versus moisture water content for different densities.

voids between fibers lead to an increase in heat capacity due to the heat mass storage of fibers. For a given density, as shown in Fig. 16, the heat capacity increases with the water content due to the higher heat capacity of water [3].

4.2.2. Effect of mean temperature for different densities on heat capacity

The effect of temperature on the heat capacity of dry fibers with various densities and arrangements was analyzed. The evolution of heat capacity as a function of temperature for random and longitudinal arrangements is illustrated in Fig. 17 and Fig. 18. A linear relationship of heat capacity versus temperature, as presented by Eq. 7, was observed. Two slopes were defined for the corresponding linear relations: 0.0038 W/m and 0.012 W/m for random and longitudinal arrangements of fibers, respectively. Similar behavior is observed with thermal conductivity, as described in Section II. 1. 1. 2.

$$c = c_0(1 + b'T) \tag{7}$$

- c_0: heat capacity at initial temperature of fibers
- $b' = \frac{a'}{c_0}$ [K]
- For random arrangement fibers case: a' = 0.0038 W/m
- For longitudinal arrangement fibers case: a' = 0.012 W/m

The results obtained in this study regarding the evolution of the heat capacity of fibers as a function of temperature are in good agreement with those observed by Yousefi & Tariku (2021) for other insulating materials. A comparison of the thermal heat capacity of random and longitudinal fibers for different densities, such as 100 and 400 kg/m^3, can be observed in Fig. 19.a and Fig. 19.b, revealing that longitudinal fibers exhibit higher heat capacity than random fibers. This can be attributed to the fact that in the case of a random arrangement, flax fibers are in closer contact compared to longitudinal ones. The heat capacity of air is approximately 1.2 MJ/ (m^3. K) when the temperature ranges between 293.15 and 303.15 K [48], whereas for the same temperature range, the thermal capacity of fibers does not exceed 0.9 MJ/ (m^3. K). Therefore, it is shown that the greater the presence of air between fibers, the greater the heat storage capacity of the fibers.

5. Raw earth-fibers composite material

5.1. Effect of moisture, water content, and fibers content on the thermal conductivity of the composite

In this section, the thermal conductivity of the composite silty-sand-random flax fibers as a function of water content was measured for 0%, 1%, and 3% fibers contents. The physical properties of the silty-sand-flax fibers samples are listed in Table 3. Fig. 20 illustrates that the thermal conductivity increases with the increase in saturation degree of the

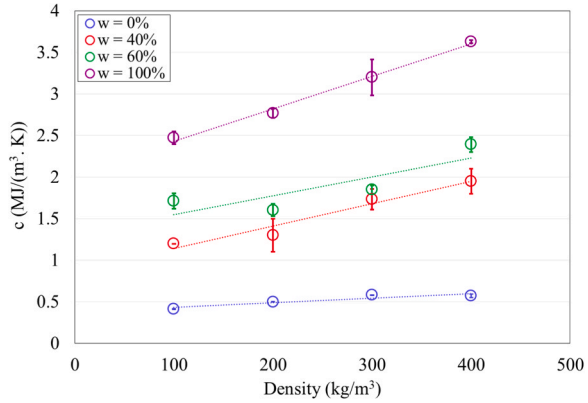

Fig. 16. Heat capacity of flax fibers versus fibers density.

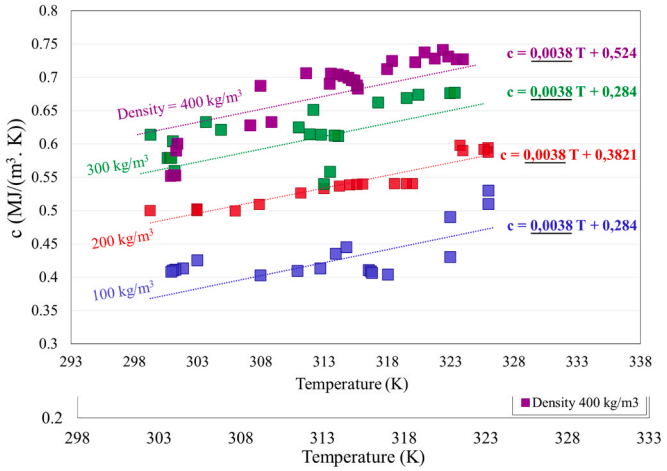

Fig. 17. Heat capacity evolution versus temperature for random arrangement.

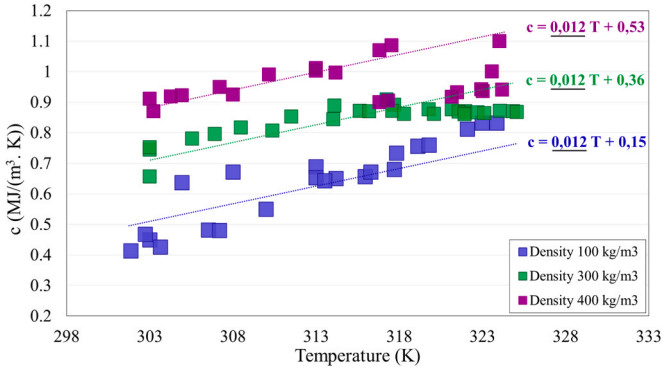

Fig. 18. Heat capacity evolution versus temperature for longitudinal arrangement.

samples and tends toward a plateau when the composite tends to a saturation threshold. The R^2 coefficients obtained for the thermal conductivity evolution curves as a function of saturation degree of raw earth with 0%, 1%, and 3% of fibers is 0.9907, 0.9911 and 0.9845, respectively. As previously observed with the effect of water on thermal conductivity, in this case as well, the thermal conductivity increases from 0.6 W/ (m. K) to 1.85 W/ (m. K) as the saturation degree increases from 0 (dry) to 1 (saturated). This can be attributed to the significant difference between the thermal conductivities of water and void air, where λ_{water} = 0.62 W/ (m. K), λ_{air} = 0.025 W/ (m. K), [29]). Consequently, wetted flax fibers conduct heat more effectively than dried fibers. Moreover, in the soil-fibers composite, the presence of fibers can enhance the insulation properties of the material. This is because the flax fibers are less heat-conductive than the silty sand.

5.2. Effect of moisture, water content, and fibers content on the heat capacity of the composite

The heat capacity of the silty-sand alone and reinforced with 1% and 3% fibers content was analyzed at various moisture contents and saturation degrees. The results of the heat capacity were plotted as a function of the degree of saturation, as shown in Fig. 21. It was anticipated that increasing the percentage of fibers would enhance the heat storage capacity. However, for the limited studied cases, the expected conclusion appears not to be clearly achieved. Additionally, the heat capacity increases with the degree of saturation. For instance, in the case of a fibers content of 1%, the heat capacity increases from 1.47 to 3.08 MJ/ (m^3. K). Regarding the previous research results in the literature, the results

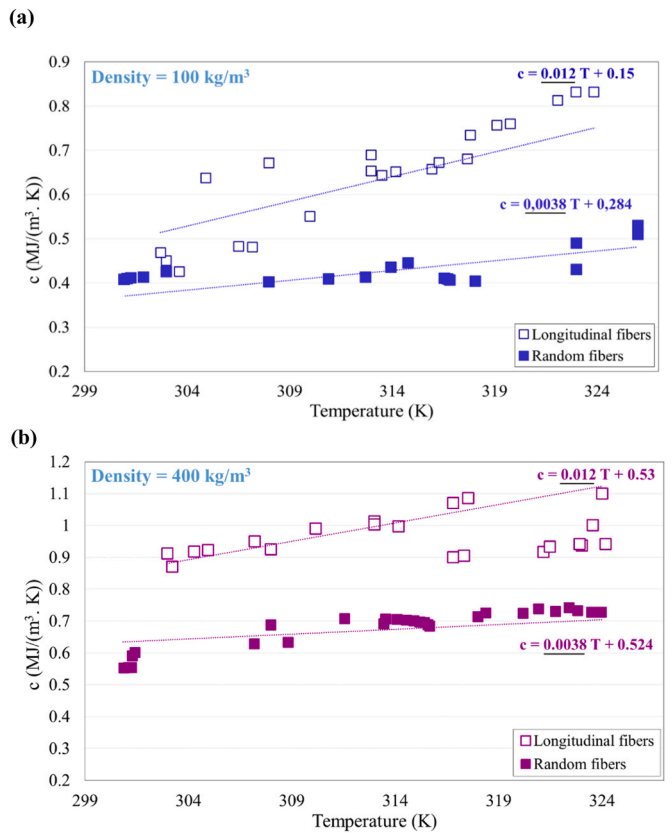

Fig. 19. Comparison of heat capacity-temperature results of random and longitudinal fibers for densities: **(a)** 100 kg/m^3 and **(b)** 400 kg/m^3.

Table 3
Properties of silty sand-flax fibers samples.

Sample	Dry density γ_d (kN/m^3)	Porosity (%)	Saturated water content w_{sat} (%)
Silty sand- 0% flax fibers	17	33	20
Silty sand- 1% flax fibers	16.5	37	23
Silty sand- 3% flax fibers	15.6	40	26

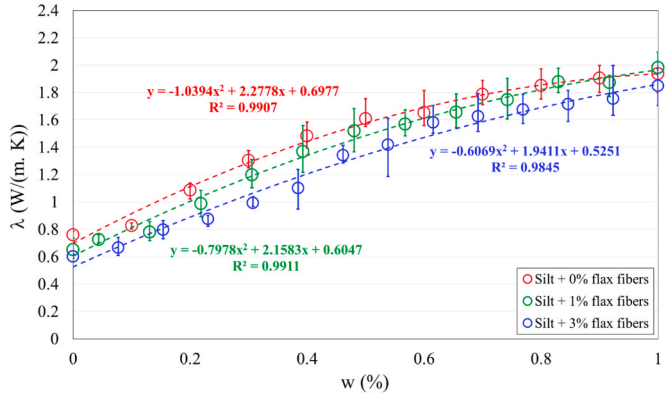

Fig. 20. Silty-sand-flax fibers thermal conductivity evolution as a function of degree of saturation.

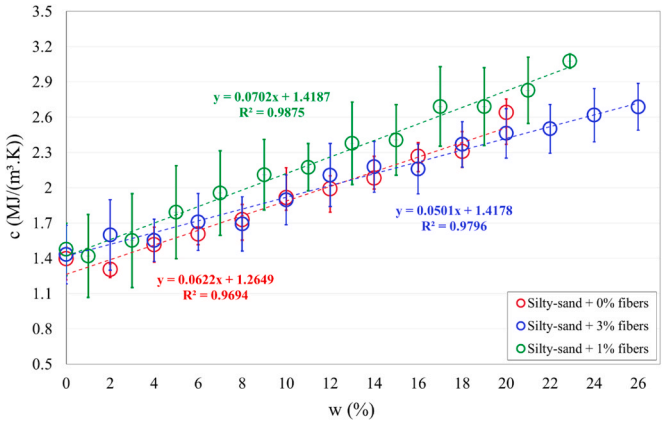

Fig. 21. Silty-sand-flax fibers heat capacity versus degree of saturation.

of this study are in agreement with other results about the effect of water content on the heat storage capacity of porous building materials (see, for instance, [26,20]).

6. Discussion

A review of the literature reveals that various authors have explored the thermal properties of fibers alone, raw earth alone, or raw earth-vegetal fibers composites. Tables 4 and 5 provide a summary of the key findings from some published papers. The studies differ in terms of the density ranges examined, the types of fibers arrangements considered, and the devices used for measuring thermal properties. For instance, Vaitkus [46] reported that chopped and long flax fibers have thermal conductivities ranging from 0.052 to 0.045 W/ (m. K.) and from 0.044 to 0.034 W/ (m. K.), respectively, for fibers densities ranging from 40 to 100 kg/m^3. Moreover, Abbas et al. [1] demonstrated that the thermal conductivities of hemp and sunflower fibers are 0.07 and 0.05 W/ (m. K), respectively, for densities of 100 and 14 kg/m^3. After comparing the thermal conductivity and heat capacity results of flax fibers with those reported in the literature for other types of plant fibers (Table 4), it is evident that they are within the same order of magnitude.

In this study, the thermal conductivity of flax fibers was obtained in the ranges between 0.041 and 0.067 W/ (m. K) and for the heat capacity it ranges from 0.39 to 1.1 MJ/ (m^3. K). The values obtained was in the

Table 4
Thermal conductivity of different vegetal fibres alone, provided from some literature references.

Vegetal fibers	Reference	Density [kg/ m^3]	λ [W/ (m. K)]	c [MJ/ (m3. K)]
Straw	[23]	440	0.18	0.396
Hemp shiv	[12]	420	0.13	0.699
Chopped flax fibers	Vaitkus [46]	40 – 100	0.052 – 0.045	-
Combed longue flax fibers			0.044–0.034	-
Bamboo	[27]	70 – 170	0.042–0.052	-
Typha	[40]	304–586	0.065 – 0.112	0.277 – 0.563
Rape straw (RS)	[10]	64.9	0.043	-
Sunflower stem (SP)		129.3	0.053	-
Sunflower bark (SB)		15.9	0.036	-
Coconut fibers	[11]	30 – 120	0.02–0.054	-
Hemp shiv	[14]	99.6 – 122.4		1.23–1.42
Hemp	[1]	100	0.07	-
Sunflower		14	0.05	-
Flax fibers	*Current study*	*100–400*	*0.041 – 0.067*	*0.39 – 1.1*

Table 5
Thermal conductivity and heat capacity of different raw-earth alone and raw earth-composite materials.

	Raw earth-based materials	Reference	Soil contents (%)	Type and amount of fibers by mass	Dry density [kg/ m^3]	λ [W/ (m. K)]	c [MJ/ (m^3. K)]
Raw earth alone	Rammed earth	Hall & Allison., 2009	30% Clay, 0–30% Sand and 40–70% Gravel	-	1980–2120	0.833–1.01	-
	Unfired earth bricks	[5]	28.7% Clay, 63.3% Silt, 5% Sand and 3% Gravel		1089 – 1577	0.31–0.96	-
	Unfired earth bricks	[37,36]	-	-	1761–1797	0,77–0,95	1.44 – 1.577
	Compressed earthen bricks	[28]	20% Clay, 61% Silt and 19% Sand	-	1940	1.1	1.82
	Compressed earthen bricks	[50]	17% Clay, 51% Silt and 32% Sand	-	1500–2000	0.52–0.93	-
	Earth slip	[14]	Earth slip	-	-	-	0.765 – 0.925
Raw earth – vegetal fibers	Raw earth concrete	[26]		-	-	0.4–1.4	1.5–2.9
	Adobe	[39]	25% Clay, 30% Silt and 45% Sand	Hibiscus cannibinus 0%, 0.2%, 0.4% and 0.8%	-	1.30–1.67	-
	Unfired earth bricks	[22]	50% Clay, 38% Silt and 12% Sand	Straw 0%, 3% and 6%	1075–1995	0.14–0.57	-
	Adobe	[41]	56% Clay, 14% Silt and 30% Sand	Fonio straw 0%, 0.2%, 0.4%, 0.6%, 0.8% and 1%	-	0.37–1.05	-
	Cob	[42]	26.7% Gravel, 40.5% Sand and 32.8% de Silt	Straw 0%, 1%, 2% and 3%	1400–1750	0.625–1.65	-
	Light earth	[14]	Earth slip	Hemp shiv	195–345	0.06 – 0.1	0.187 – 0.38
	Cob	[6]	-	Flax straw 2.5%	1650–2000	0.5–1.3	-
	Sandy-silt – flax fibers	*Current study*	*25% Silt, 67% Sand and 8% Gravel*	*Flax fibers 0%, 1% and 3%*	*1560–1700*	*0.6–0.76*	*1.4–3.08*

minimum, and maximum ranges reported in the literature for various studied fibers. For materials based on raw earth (Table 5), Hall & Allinson [24] demonstrated that for a density ranging from 1980 to 2120 kg/m^3, thermal conductivity varies from 0.833 to 1.01 W/ (m. K), respectively. In the case of raw earth-vegetal fibers, Phung et al. [42] observed that thermal conductivity ranges from 0.625 to 1.65 W/ (m. K), for a density range of 1400–1750 kg/m^3. Azil et al. [6] demonstrated that, for cob, for density variations from 1650 to 2000 kg/m^3, the thermal conductivity ranges from 0.5 to 1.3 W/ (m. K). The heat capacity of the silty-sand-flax fibers ranges from 1.4 to 3.08 MJ/ (m^3. K) which was in a good agreement in a comparison of minimum and maximum values in the literature, ranges between 0.187 and 2.9 MJ/ (m^3. K), respectively.

The results presented in this study for the silty-sand-flax fibers composite are globally in agreement with the other raw earth-vegetal fibers composites. However, the comparison with the other published studies and the corresponding results was only possible "qualitatively." Published results were found to be in accordance with those of other studies regarding densities of fibers, types of arrangement and distribution of fibers, measuring devices, and preparation or conditioning specimens. Many of these studies include a wide range of fibers.

Published studies demonstrate that fibers significantly influencing the thermal conductivity and sorption capacity of earthen materials which cannot be ignored. Recently, fibers were used in various applications and studied both numerically and experimentally in the laboratory for improving the mechanical properties. An important point that researchers recently addressed the fibers in bioengineering applications, fibers-reinforced porous media, and dispersive composite materials [16, 4]. This will bring the future view on not even as the energy savings and insulation materials but also can be applicable in bioengineering fields.

7. Conclusion

This paper focuses on the thermal properties of silty-sand-flax fibers composite building materials. Firstly, the study focused on flax fibers alone, examining the impacts of water content, temperature, arrangement, and density on their thermal properties, which were quantified through experimental methods. Subsequently, the thermal properties of the silty-sand-flax fibers materials were evaluated using the unsteady (transient) heat diffusion method. The role of water content in relation with flax fibers content was studied and the corresponding curves are given as thermal conductivity and heat capacity versus the degree of saturation. The mathematical relationships obtained from these analyses were then presented and analyzed.

Regarding the thermal properties of flax fibers alone, the main findings are summarized as follows:

- The thermal conductivity exhibits a linear relationship with temperature and water content, irrespective of sample density. For samples with a density of 400 kg/m^3, it increases from 0.067 to 0.36 W/ (m. K) as the water content varies from 0% to the saturation level (w_{sat}). This can be explained by the fact that the thermal conductivity of water is higher than that of dry fibers. Moreover, it increases with temperature, indicating that temperature enhances heat diffusion. This finding is well known as the heat transfer phenomenon. However, in this paper, the quantification of this linear dependency was achieved through an intrinsic coefficient, represented by the slope of the linear curves. This coefficient serves to characterize the relationship between the heat conductivity of flax fibers and the temperature, independent of the density and the arrangement.
- The heat capacity depends on the density of fibers, their arrangement, and their temperature and water content initial conditions. The effect of these parameters on heat capacity exhibited a similar trend to that observed for thermal conductivity. A linear equation, characterized by slopes of 0.0038 W/m for random arrangements and 0.012 W/m for longitudinal arrangements, was recognized for heat capacity as a function of temperature. Additionally, longitudinally arranged fibers show a higher heat storage capacity than random arrangements.
- A comparison of the thermal conductivity and heat capacity obtained in this study shows a good agreement with the minimum and maximum values of the literature.

Regarding the silty-sand-flax fibers composite, the main conclusions can be summarized as follows:

- The thermal conductivity increases with the increase in water content, irrespective of the percentage of added fibers. For 3% of fibers, the thermal conductivity increases from 0.6 W/ (m. K) to 1.85 W/ (m. K) as the water content increases from 0% to 26%.
- The addition of fibers to silty-sand has improved the insulating capacity of the composite material. This improvement stems from the fact that flax fibers conduct heat less effectively than silty-sand. For a water content of 14%, the thermal conductivity decreases from 1.786 to 1.417 W/ (m. K) as the fibers content increases from 0% to 3%.
- A comparison of the thermal properties of silty-sand-flax fibers with those of raw earth-vegetal fibers building materials observed in the literature highlights similar variations in thermal properties. However, the newly established mathematical relationships present new findings to be considered for future fabrication and study of building material-fibers composites.
- The heat capacity of the composite material did not show a significant difference when examining various percentages of fibers, ranging from 0% (silt alone without fibers) to 1% and 3% of fibers. However, a linear trend was observed for heat capacity as the degree of saturation increased, irrespective of the fibers content.
- The relationships between thermal properties and temperature, as well as saturation degree, showed the beneficial impact of fibers in improving the thermal behavior and heat transfer of the composite silty-sand-flax fibers. This finding warrants further examination with other fibers contents, different types of fibers, and other bio-source binder materials. Notably, such research endeavors should also consider optimizing the added fibers content or other bio-source material to ensure the required mechanical properties.

CRediT authorship contribution statement

Abdelkader Mabrouk: Writing – review & editing, Validation. **Mehrez Jamei:** Writing – review & editing, Validation, Supervision, Resources, Project administration, Funding acquisition. **Said Taibi:** Writing – review & editing, Validation, Supervision, Resources, Project administration, Funding acquisition, Conceptualization. **Tariq OUAHBI:** Writing – review & editing, Validation, Supervision, Methodology, Investigation, Conceptualization. **Habib Jalili:** Writing – review & editing, Validation, Investigation, Formal analysis, Data curation. **Ichrak Hamrouni:** Writing – original draft, Validation, Methodology, Investigation, Formal analysis, Data curation, Conceptualization.

Declaration of Competing Interest

The authors declare that they have no known competing financial interests or personal relationships that could have appeared to influence the work reported in this paper.

Data availability

Data will be made available on request.

Acknowledgements

1) The authors extend their appreciation to the Deanship of Scientific Research at Northern Border University, Arar, KSA for funding this research work through the project number “NBU-FFR-2024–2740–02”

2) The authors express their gratitude to the Tunisian government and the University of Le Havre Normandy for providing financial support. Additionally, they appreciate the funding received from their Deputyship for Research & Innovation at the Ministry of Education (France) for the achievement of this research project.

References

[1] M.-S. Abbas, E. Gourdon, Ph Glé, F. McGregor, Ferroukhi, M-YAntonin Fabbri, Relationship between hygrothermal and acoustical behavior of hemp and sunflower composites, Build. Environ. 188 (2021) 107462, https://doi.org/10.1016/j.buildenv.2020.107462.

[2] M. Abramowitz, I.A. Stegun (Eds.), Handbook of mathematical functions with formulas, graphs, and mathematical tables, Vol. 55, US Government printing office, 1968.

[3] N.H. Almousa, M.R. Alotaibi, M. Alsohybani, D. Radziszewski, S.M. AlNoman, B. M. Alotaibi, M.M. Khayyat, Paraffin wax [as a phase changing material (Pcm)] based composites containing multi-walled carbon nanotubes for thermal energy storage (tes) development, Crystals 11 (8) (2021) 951, https://doi.org/10.3390/cryst11080951.

[4] A. Amendola, J. de CastroMotta, G. Saccomandi, L. Vergori, Constitutive model for transversely isotropic dispersive materials, Proc. R. Soc. A480 (2024) 20230374, https://doi.org/10.1098/rspa.2023.0374.

[5] T. Ashour, A. Korjenic, S. Korjenic, W. Wu, Thermal conductivity of unfired earth bricks reinforced by agricultural wastes with cement and gypsum, Energy Build. 104 (2015) 139–146, https://doi.org/10.1016/j.enbuild.2015.07.016.

[6] O. Azil, K. Touati, N. Sebaibi, M. Le Guern, F. Streiff, S. Goodhew, M. Gomina, M. Boutouil, Monitoring of drying kinetics evolution and hygrothermal properties of new earth-based materials using climatic chamber simulation, Case Stud. Constr. Mater. 18 (2022) e01798, https://doi.org/10.1016/j.cscm.2022.e01798.

[7] M. Ben Mansour, A. Jelidi, A.-S. Cherif, S. Ben Jabrallah, Optimizing thermal and mechanical performance of compressed earth blocks (CEB), Constr. Build. Mater. 104 (2016) 44–51, https://doi.org/10.1016/j.conbuildmat.2015.12.024.

[8] S. Bouchemella, Thème: Contribution à la Simulation Numérique des Ecoulements Des Eaux Dans les Milieux Poreux Non Saturés [Theme: Contribution to Numerical Simulation of Water Flow in Unsaturated Porous Media], Université de Guelma, Algeria, 2015 (PhD Thesis).

[9] A.W. Bruno, Hygro-mechanical characterisation of hypercompacted earth for building construction (PhD Thesis), University of Pau and Pays de l'Adour, 2016.

[10] Y. Brouard, N. Belayachi, D. Hoxha, N. Ranganathan, S. Méo, Mechanical and hygrothermal behavior of clay – Sunflower (Helianthus annuus) and rape straw (Brassica napus) plaster bio-composites for building insulation, Constr. Build. Mater. 161 (2018) (2018) 196–207, https://doi.org/10.1016/j.conbuildmat.2017.11.140.

[11] Bui, H., Sebaibi, N., Boutouil, M., Levacher, D. Determination and Review of Physical and Mechanical Properties of Raw and Treated Coconut Fibers for Their Recycling in Construction Materials. Fibers 8(6), 37. ⟨https://doi.org/10.3390/fib8060037⟩.

[12] R. Busbridge, R. Rhydwen, An investigation of the thermal properties of hemp and clay monolithic walls. Proceedings of Advances in Computing and Technology, (AC&T) The School of Computing and Technology 5th Annual Conference, University of East London, 2010.

[13] M. Chabannes, V. Nozahic, S. Amziane, Design and multi-physical properties of a new insulating concrete using sunflower stem aggregates and eco-friendly binders, Mater. Struct. /Mater. Et. Constr. 48 (6) (2015) 1815–1829, https://doi.org/10.1617/s11527-014-0276-9.

[14] T. Colinart, T. Vinceslas, H. Lenormand, A.H. De Menibus, E. Hamard, T. Lecompte, Hygrothermal properties of light-earth building materials, J. Build. Eng. 29 (2020) 101134, https://doi.org/10.1016/j.jobe.2019.101134.

[15] K. Daryabeigi, G.-R. Cunnington, J.-R. Knutson, Combined heat transfer in high-porosity high-temperature fibrous insulation: theory and experimental validation, J. Thermophys. Heat. Tran. 25 (4) (2011) 536–546, https://doi.org/10.2514/1.T3616.

[16] J. De Castro Motta, V. Zampoli, S. Chiriță, M. Ciarletta, On the structural stability for a model of mixture of porous solids, Math. Methods Appl. Sci. (2023).

[17] J. Eid, S. Taibi, J.M. Fleureau, M. Hattab, Drying, cracks and shrinkage evolution of a natural silt intended for a new earth building material. Impact of reinforcement, Constr. Build. Mater. 86 (2015) 120–132, https://doi.org/10.1016/j.conbuildmat.2015.03.115.

[18] N. El Hajj, R.-M. Dheilly, A. Goullieux, Z. Aboura, M.-L. Benzeggagh, M. Quéneudec, Innovant agromaterials formulated with flax shaves and proteinic binder: Process and characterization, Compos. Part B: Eng. 43 (2) (2012) 381–390, https://doi.org/10.1016/j.compositesb.2011.05.022.

[19] A. El Hajjar, T. Ouahbi, S. Taibi, J. Eid, M. Hattab, J.M. Fleureau, Assessing crack initiation and propagation in flax fiber reinforced clay subjected to desiccation, Constr. Build. Mater. 278 (2021) 122392, https://doi.org/10.1016/j.conbuildmat.2021.122392.

[20] M.Y. Ferroukhi, R. Belarbi, K. Limam, A. Si Larbi, A. Nouviaire, Assessment of the effects of temperature and moisture content on the hygrothermal transport and storage properties of porous building materials, Heat. Mass Transf. 55 (2019) 1607–1617, https://doi.org/10.1007/s00231-018-02550-5.

[21] D. Gallipoli, A.W. Bruno, C. Perlot, J. Mendes, A geotechnical perspective of raw earth building, Acta Geotech. 12 (2017) 463–478, https://doi.org/10.1007/s11440-016-0521-1.

[22] M. Giroudon, A. Laborel-Préneron, J.-E. Aubert, C. Magniont, Comparison of barley and lavender straws as bioaggregates in earth bricks, Constr. Build. Mater. 202 (2019) 254–265, https://doi.org/10.1016/j.conbuildmat.2018.12.126.

[23] S. Goodhew, R. Griffiths, Sustainable earth walls to meet the building regulations, Energy Build. 37 (5) (2005) 451–459, https://doi.org/10.1016/j.enbuild.2004.08.005.

[24] M. Hall, D. Allinson, Analysis of the hygrothermal functional properties of stabilised rammed earth materials, Build. Environ. 44 (2009) 1935–1942, https://doi.org/10.1016/j.buildenv.2009.01.007.
[25] I. Hamrouni, T. Ouahbi, A. El Hajjar, S. Taibi, M. Jamei, H. Zenzri, Water vapor permeability of flax fibers reinforced raw earth: experimental and micro-macro modeling, Eur. J. Environ. Civ. Eng. 27 (10) (2023) 3020–3039, https://doi.org/10.1080/19648189.2022.2123857.
[26] A. Hibouche, Sols traites aux liants Performances hydro-mecaniques et hygro-thermiques Applications en BTP [Soils treated with binders Hydro-mechanical and hygro-thermal performance Construction applications] (PhD thesis), University of Le Havre, 2013.
[27] Z. Huang, Y. Sun, F. Musso, Hygrothermal performance of natural bamboo fiber and bamboo charcoal as local construction infills in building envelope, Constr. Build. Mater. (2018), https://doi.org/10.1016/j.conbuildmat.2018.05.071.
[28] M. Indekeu, M. Woloszyn, A.C. Grillet, L. Soudani, A. Fabbri, Towards Hygrothermal characterization of rammed earth with small-scale dynamic methods, Energy Procedia 132 (2017) 297–302, https://doi.org/10.1016/j.egypro.2017.09.731.
[29] H. Kallel, Influence de la température et de l'hygrométrie sur le comportement instantané du béton [Influence of temperature and hygrometry on the instantaneous behavior of concrete], University of Pau and of Pays de l'Adour, 2016 (PhD Thesis).
[30] Kh Khoukhi, N. Fezzioui, B. Draoui, L. Salah, The impact of changes in thermal conductivity of polystyrene insulation material under different operating temperatures on the heat transfer through the building envelope, Appl. Therm. Eng. 105 (2016) 669–674, https://doi.org/10.1016/j.applthermaleng.2016.03.065.
[31] J.H. Knight, G.J. Kluitenberg, T. Kamai, J.W. Hopmans, Semianalytical solution for dual-probe heat-pulse applications that accounts for probe radius and heat capacity, Vadose Zone J. 11 (2) (2012). Doi:10.2136/vzj2011.0112.
[32] M. Koru, Determination of thermal conductivity of closed-cell insulation materials that depend on temperature and density, Arab. J. Sci. Eng. 41 (11) (2016) 4337–4346, https://doi.org/10.1007/s13369-016-2122-6.
[33] Magniont, C. (2010). Contribution à la formulation et à la caractérisation d'un écomatériau de construction à base d'agroressources (Doctoral dissertation, Toulouse 3).
[34] Donald W. Marquardt, An algorithm for least-squares estimation of nonlinear parameters, J. Soc. Ind. Appl. Math. 11 (2) (1963) 431–441, https://doi.org/10.1137/0111030.
[35] B. Mazhoud, F. Collet, S. Pretot, C. Lanos, Effect of hemp content and clay stabilization on hygric and thermal properties of hemp-clay composites, Constr. Build. Mater. 300 (2021) 123878, https://doi.org/10.1016/j.conbuildmat.2021.123878.
[36] D. Medjelekh, Caractérisation multi-échelle du comportement thermo hybride des enveloppes hygroscopiques [Multi-scale characterization of the thermohybrid behavior of hygroscopic envelopes] (PhD Thesis), Université de Limoges, 2015.
[37] D. Medjelekh, L. Ulmet, F. Dubois, Characterization of hygrothermal transfers in the unfired earth, Energy Procedia 139 (2017) 487–492, https://doi.org/10.1016/j.egypro.2017.11.242.
[38] L. Miccoli, U. Müller, P. Fontana, Mechanical behaviour of earthen materials: a comparison between earth block masonry, rammed earth and cob, Constr. Build. Mater. 61 (2014) 327–339, https://doi.org/10.1016/j.conbuildmat.2014.03.009.
[39] Y. Millogo, J.C. Morel, J.E. Aubert, K. Ghavami, Experimental analysis of pressed adobe blocks reinforced with hibiscus cannabinus fibers, Constr. Build. Mater. 52 (2014) 71–78, https://doi.org/10.1016/j.conbuildmat.2013.10.094.
[40] I. Niang, Ch Maalouf, T. Moussa, Ch Bliard, E. Samin, C. Thomachot-Schneider, M. Lachi, H. Pron, T.-H. Mai, S. Gaye, Hygrothermal performance of various Typha–clay composite, J. Build. Phys. (2018) 1–20, https://doi.org/10.1177/1744259118759677.
[41] M. Ouedraogo, K. Dao, Y. Millogo, J. Aubert, A. Messan, M. Seynou, L. Zerbo, M. Gomina, Thermal and mechanical properties of adobes stabilized with fonio (Digitaria exilis) straw, J. Build. Eng. 23 (2019) 250–258, https://doi.org/10.1016/j.jobe.2019.02.005.
[42] T.-A. Phung, M. Le Guern, M. Boutouil, H. Louahlia, Hygrothermal Behaviour of Cob Material, in: B.V.V. Reddy, et al. (Eds.), Earthen Dwellings and Structures, Springer Transactions in Civil and Environmental Engineering, 2019, https://doi.org/10.1007/978-981-13-5883-8_30.
[43] S. Sangma, D.-D. Tripura, Characteristic properties of unstabilized, stabilized and fibre-reinforced cob blocks, Struct. Eng. Int. 31 (2021) 76–84. ⟨https://doi.org/10.1080/10168664.2019.1690957⟩.
[44] C.-S. Tang, B. Shi, C. Liu, W.-B. Suo, L. Gao, Experimental characterization of shrinkage and desiccation cracking in thin clay layer, Appl. Clay Sci. 52 (1) (2011) 69–77, https://doi.org/10.1016/j.clay.2011.01.032.
[45] F. Tariku, Y. Shang, S. Molleti, Thermal performance of flat roof insulation materials: A review of temperature, moisture and aging effects, J. Build. Eng. 76 (2023) 107142, https://doi.org/10.1016/j.jobe.2023.107142.
[46] S. Vaitkus, R. Karpavičiūtė, S. Vėjelis, L. Lekūnaitė, Development and research of thermal insulation materials from natural fibres, Key Eng. Mater. Vol. 604 (2014) 285–288. DOI: 10.4028/www.scientific.net/KEM.604.285.
[47] T. Vinceslas, T. Colinart, E. Hamard, A.-H. de Ménibus, T. Lecompte, H. Lenormand, Light Earth erformances for thermal insulation: application to earth–hemp, Earthen Dwell. Struct. (2017) 357–367, https://doi.org/10.1007/978–981-13–5883-8_31.
[48] Y. Wang, M. Boulic, R. Phipps, M. Plagmann, C. Cunningham, Experimental performance of a solar air collector with a perforated back plate in New Zealand, Energies 13 (6) (2020) 1415, https://doi.org/10.3390/en13061415.
[49] Y. & Yousefi, F. Tariku, Thermal conductivity and specific heat capacity of insulation materials at different mean temperatures, J. Phys.: Conf. Ser. 2069 (2021) 012090, https://doi.org/10.1088/1742-6596/2069/1/012090.
[50] L. Zhang, L. Yang, B.-P. Jelle, Y. Wang, A. Gustavsen, Hygrothermal properties of compressed earthen bricks, Constr. Build. Mater. 162 (2018) 576–583, https://doi.org/10.1016/j.conbuildmat.2017.11.163.